

Strain-induced inter-vortex interaction and vortex lattices in tetragonal superconductors

Shi-Zeng Lin¹ and Vladimir G. Kogan²

¹Theoretical Division, Los Alamos National Laboratory, Los Alamos, New Mexico 87545, USA

²Ames Laboratory, DOE and Department of Physics, Iowa State University, Ames, Iowa 50011, USA

(Dated: December 16, 2016)

In superconductors with strong coupling between superconductivity and elasticity manifested in a strong dependence of transition temperature on pressure, there is an additional contribution to inter-vortex interactions due to the strain field generated by vortices. When vortex lines are along the c axis of a tetragonal crystal, a square vortex lattice (VL) is favored at low vortex densities, because the vortex-induced strains contribution to the inter-vortex interactions is long range. At intermediate magnetic fields, the triangular lattice is stabilized. The triangular lattice evolves to the square lattice upon increasing magnetic field, and eventually the system locks to the square structure. We argue, however, that as B approaches H_{c2} the elastic inter-vortex interactions disappear faster than the standard London interactions, so that VL should return to the triangular structure. Our results are compared to VLs observed in the heavy fermion superconductor CeCoIn₅.

I. INTRODUCTION

Vortices are topological excitations in superconductors under magnetic field and they organize in periodic lattices due to the mutual interaction. In isotropic superconductors, the vortices form hexagonal lattices stabilized by the repulsive magnetic interaction. The energy difference between triangular and square lattices are extremely small [1], therefore the VLs are sensitive to higher order interaction terms. It was shown that VL evolves from a triangular to a square lattice upon increasing magnetic field in tetragonal non-magnetic borocarbides due to nonlocality of the relation between supercurrent and vector potential and the Fermi surface anisotropy [2]. Square lattice is also favored in high- T_c superconductors when both the s - and d -wave components are present [3].

A vortex can perturb the strain field of the crystal that induces additional interactions between vortices [4–9]. In a simple picture, nucleation of the normal vortex core which has a different density than the surrounding superconductor, induces a strain field. This strain decays as a power of the distance from the vortex core and mediates long-range interaction between vortices. The strain-induced interaction follows the crystal symmetry. For instance, for vortices directed along the c axis in tetragonal crystal, the strain-induced interaction has four-fold rotational symmetry in the ab plane. It is shown below that because of the long-range nature, the strain-induced interaction, its weakness notwithstanding, dominates over the short-range magnetic interaction at very small vortex densities (or low magnetic inductions B) and at sufficiently high vortex densities where the elastic part of the free energy increases as B^2 , whereas the standard magnetic interaction scales as B .

The coupling between superconductivity and elasticity is characterized by the rate of change of the critical temperature T_c with respect to stress/pressure p , i.e. by derivatives dT_c/dp . It was argued in Ref. [4] that in NbSe₂ with $dT_c/dp \approx 0.5$ K/GPa, the magneto-elastic interactions might be responsible for observed VL structures. In a heavy-fermion superconductor CeCoIn₅, $dT_c/dp \approx 0.3$ K/GPa. For iron-based materials, dT_c/dp is on the order of K/GPa and varies with doping. In some of those, e.g. in Ca(Fe_{1-x}Co_x)₂As₂,

$dT_c/dp \approx -60$ K/GPa which is by two orders of magnitude larger than common values [10]. Hence, all these materials are good candidates for observing the vortex structure evolution and transitions caused by strain induced interactions.

The elastic contribution to intervortex interaction in tetragonal materials has been discussed in Ref. 6. However, the VL structures in the presence of the new interaction have not been studied. The present work aims to fill this gap. We will also discuss the possible relevance of strain-induced interaction to the VL transitions observed by small angle neutron scattering in CeCoIn₅ [11–13].

II. MODEL

Within our model, the total energy density F associated with the VL consists of the superconducting contribution F_m and the elastic energy density

$$F_e = \lambda_{iklm} u_{ik} u_{lm} / 2, \quad (1)$$

where λ_{iklm} are elastic moduli and u_{ik} are strains. Summation over repeated indices is implied throughout the paper. We will focus on tetragonal crystals. For brevity we denote the six independent moduli in the crystal frame (a, b, c) as: $\lambda_{aaaa} = \lambda_{bbbb} = \lambda_1$, $\lambda_{aabb} = \lambda_2$, $\lambda_{abab} = \lambda_3$, $\lambda_{cccc} = \lambda_4$, $\lambda_{aacc} = \lambda_{bbcc} = \lambda_5$ and $\lambda_{acac} = \lambda_{bcbc} = \lambda_6$ [14].

Within the London approximation, we have for the magnetic and kinetic parts of the superconducting free energy density [15, 16]:

$$8\pi F_m = \mathbf{h}^2 + \lambda_L^2 m_{ik} (\nabla \times \mathbf{h})_i (\nabla \times \mathbf{h})_k. \quad (2)$$

where \mathbf{h} is the local magnetic field, the mass tensor m_{ik} accounts for the uniaxial anisotropy, and λ_L is the geometric average of the penetration depths.

We take the Bardeen-Stephen approximation for the vortex core as a normal region of size of ξ [17]. The crystal expands or shrinks in the normal region: $(V_n - V_s)/V_s = H_c \partial_p H_c / 4\pi$, where $V_{n,s}$ are the specific volumes of the normal and superconducting phases, p is the pressure, and H_c is the thermodynamic critical field [18]. One can consider the vortex as a

point source, which induces the strain field [4]. This London-type model is, of course, oversimplified and works far from the upper critical field $H_{c2}(T)$ and for $\lambda_L \gg \xi$.

Let vortex lines be directed along the unit vector $\mathbf{l} = (\cos \varphi \sin \theta, \sin \varphi \sin \theta, \cos \theta)$ in the tetragonal crystal frame (θ is the angle between \mathbf{c} and \mathbf{l} , φ is the angle between the a axis and the projection of \mathbf{l} onto the ab plane). We introduce also the “vortex frame” (X, Y, Z) such that the Z direction is along the vortex line. A vector \mathbf{V} in the rotated frame is related to the vector \mathbf{v} in the crystal frame by a rotation $\mathbf{v} = \hat{\mathbf{O}}\mathbf{V}$, with

$$\hat{\mathbf{O}} = \begin{pmatrix} -\sin \varphi & -\cos \theta \cos \varphi & \cos \varphi \sin \theta \\ \cos \varphi & -\cos \theta \sin \varphi & \sin \theta \sin \varphi \\ 0 & \sin \theta & \cos \theta \end{pmatrix}. \quad (3)$$

The strain tensor u_{ik} in the crystal frame is related to that $U_{\alpha\beta}$, with $\alpha, \beta = X, Y, Z$, in the rotated frame according to

$$u_{ik} = \frac{1}{2} (O_{i\alpha} O_{k\beta} + O_{k\alpha} O_{i\beta}) U_{\alpha\beta}, \quad (4)$$

and the elastic moduli $\Lambda_{\alpha\beta\gamma\eta}$ in the rotated frame are

$$\Lambda_{\alpha\beta\gamma\eta} \equiv \frac{\lambda_{iklm}}{4} (O_{i\alpha} O_{k\beta} + O_{k\alpha} O_{i\beta}) (O_{l\gamma} O_{m\eta} + O_{m\gamma} O_{l\eta}). \quad (5)$$

The stress tensor $\sigma_{\alpha\beta}$ is

$$\sigma_{\alpha\beta} = \partial F_e / \partial U_{\alpha\beta} = \Lambda_{\alpha\beta\gamma\eta} U_{\gamma\eta}. \quad (6)$$

It is argued in Ref. [6] that for the vortex orientation \mathbf{l} along the principal crystal directions, the problem of elastic perturbation caused by straight vortices can be considered as *planar*, i.e. the deformations $\mathbf{U} \perp \mathbf{l}$ everywhere and the strains $U_{aZ} = 0$. The elasticity problem then simplifies considerably, and below we consider two vortex orientations: $\mathbf{l} \parallel \mathbf{c}$ and $\mathbf{l} \perp \mathbf{c}$. In the first case the vortex frame coincides with the crystal frame, the corresponding elastic moduli are listed above. The elastic moduli in the second case are compiled in Appendix A. In both cases, we have $\Lambda_{XXXY} = \Lambda_{XXYX} = \Lambda_{YYXY} = \Lambda_{YYXX} = \Lambda_{ZZXY} = \Lambda_{ZZYX} = 0$.

As always in planar problems, the components of the stress tensor are not independent [14]. After a simple algebra, one can exclude $U_{\gamma\eta}$ from Eqs. (6) to obtain:

$$\sigma_{ZZ} = \left(\frac{D_2}{d} - 1 \right) \sigma_{XX} + \left(\frac{D_1}{d} - 1 \right) \sigma_{YY}, \quad (7)$$

$$D_1 = d + \Lambda_{ZZYY} \Lambda_{XXXX} - \Lambda_{ZZXX} \Lambda_{XXYY}, \quad (8)$$

$$D_2 = d + \Lambda_{ZZXX} \Lambda_{YYYY} - \Lambda_{ZZYY} \Lambda_{XXYY}, \quad (9)$$

$$d = \Lambda_{XXXX} \Lambda_{YYYY} - \Lambda_{XXYY}^2. \quad (10)$$

Equilibrium conditions $\partial \sigma_{\alpha\beta} / \partial X_\beta = 0$ read:

$$\frac{\partial \sigma_{XX}}{\partial X} + \frac{\partial \sigma_{XY}}{\partial Y} = 0, \quad \frac{\partial \sigma_{YX}}{\partial X} + \frac{\partial \sigma_{YY}}{\partial Y} = 0. \quad (11)$$

The solution can be written as

$$\sigma_{XX} = \frac{\partial^2 \chi}{\partial Y^2}, \quad \sigma_{YY} = \frac{\partial^2 \chi}{\partial X^2}, \quad \sigma_{XY} = -\frac{\partial^2 \chi}{\partial X \partial Y}, \quad (12)$$

with an arbitrary function $\chi(X, Y)$ [14].

Using the condition $\sigma_{\alpha\alpha} = -3p$, we obtain for $\chi(X, Y)$:

$$\frac{D_1}{d} \frac{\partial^2 \chi}{\partial X^2} + \frac{D_2}{d} \frac{\partial^2 \chi}{\partial Y^2} = -3p. \quad (13)$$

To calculate the stress field induced by a vortex in otherwise unrestrained sample, we note that the pressure $p = 0$ while the vortex can be considered as a singular source of the stress field [6]. Because the stress field is long-ranged, we can approximate the source term using a delta function, $2\pi S_0 \delta(\mathbf{R} - \mathbf{R}_v)$ with $\mathbf{R}_v = (X_v, Y_v)$ being the vortex position [6]. Equation (13) with a delta-source can be solved by the two-dimensional Fourier transform, and both $\sigma_{\alpha\beta}(\mathbf{R}_v, \mathbf{k})$ and $U_{\alpha\beta}(\mathbf{R}_v, \mathbf{k})$ can be calculated.

The elastic contribution to the interaction energy (per unit length) of a vortex at the origin and another one at \mathbf{R}_v is

$$\mathcal{E}_e(\mathbf{R}_v) = \int \frac{d^2 \mathbf{k}}{4\pi^2} \sigma_{\alpha\beta}(0, \mathbf{k}) U_{\alpha\beta}(\mathbf{R}_v, -\mathbf{k}). \quad (14)$$

For VL along the c axis, $\theta = 0$, $D_1 = D_2 = D$, the strain induced interaction becomes

$$\begin{aligned} \mathcal{E}_e(\mathbf{R}_v) &= \left(\frac{S_0}{D} \right)^2 d \left(\lambda_1 + \lambda_2 - \frac{d}{2\lambda_3} \right) \int d^2 \mathbf{k} \frac{k_X^4 + k_Y^4}{k^4} e^{-i\mathbf{k} \cdot \mathbf{R}_v} \\ &= \left(\frac{S_0}{D} \right)^2 \frac{\pi d}{R_v^2 \lambda_3} (\lambda_1 + \lambda_2) (2\lambda_3 - \lambda_1 + \lambda_2) \cos(4\phi), \end{aligned} \quad (15)$$

where the azimuth of the second vortex position is $\phi = \tan^{-1}(Y_v/X_v)$. The interaction decays as $1/R_v^2$ and has four-fold rotational symmetry. When $2\lambda_3 - \lambda_1 + \lambda_2 > 0$, the elastic interaction changes from repulsion at $\phi = 0$ to attraction at $\phi = \pi/4$.

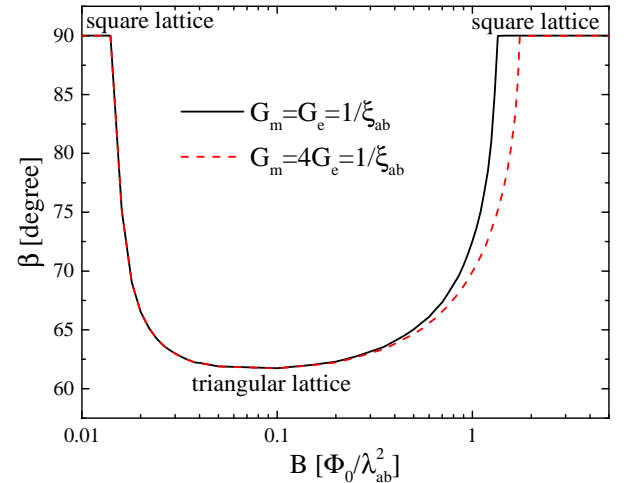


FIG. 1. (color online) The equilibrium apex angle β of the rhombic unit cell for vortex lines along c . Vortices form a square lattice both at low and high fields, and the VL is triangular at intermediate fields. For comparison, the results for two different G_e 's are displayed. The field at the transition from the triangular to square VL at higher field increases when G_e is reduced.

For VL along the ab plane, the straightforward algebra results in

$$\begin{aligned}\mathcal{E}_e(\mathbf{R}_v) &= \left(\frac{dS_0}{D_2}\right)^2 \int d^2\mathbf{k} e^{-i\mathbf{k}\cdot\mathbf{R}_v} \frac{f_X(D_1 D_2^{-1} k_X^2) + f_Y k_Y^4}{(D_1 D_2^{-1} k_X^2 + k_Y^2)^2} \\ &= \left(\frac{dS_0}{D_2}\right)^2 \frac{\pi \sqrt{D_2 D_1^{-1}}}{X_v^2 D_2 D_1^{-1} + Y_v^2} [f_+ \cos(4\phi') + 2f_- \cos(2\phi')],\end{aligned}\quad (16)$$

where

$$f_X = \frac{\Lambda_{XXXX}}{d} - \left(\frac{1}{\Lambda_{XYXY}} - \frac{2\Lambda_{XXYY}}{d}\right) \frac{D_2}{2D_1}, \quad (17)$$

$$f_Y = \frac{\Lambda_{YYYY}}{d} - \left(\frac{1}{\Lambda_{XYXY}} - \frac{2\Lambda_{XXYY}}{d}\right) \frac{D_2}{2D_1}, \quad (18)$$

$$f_{\pm} = f_Y \pm f_X, \quad \phi' = \tan^{-1} \left(\sqrt{D_1 D_2^{-1}} Y_v / X_v \right). \quad (19)$$

This interaction has the two-fold rotational symmetry. The strain induced interaction depends on the vortex orientation through $\Lambda_{\alpha\beta\gamma\eta}(\varphi)$.

III. VORTEX LATTICES

By minimizing the total interaction energy we obtain the equilibrium VL configuration. For vortices along the c axis, the lattice unit cell is a rhombus. We consider two vortex configurations with the rhombus diagonal either along $[100]$ or $[110]$ directions. The unit cell vectors of the reciprocal lattice with the rhombus diagonal in $[100]$ are

$$\mathbf{G}_{1,2} = \frac{2\pi}{a \sin \beta} \left[\sin\left(\frac{\beta}{2}\right) \hat{x} \pm \cos\left(\frac{\beta}{2}\right) \hat{y} \right]. \quad (20)$$

For the rhombus diagonal in $[110]$, we have

$$\mathbf{G}_{1,2} = \frac{2\pi}{a \sin \beta} \left[\sin\left(\frac{\beta}{2} \mp \frac{\pi}{4}\right) \hat{x} \pm \cos\left(\frac{\beta}{2} \mp \frac{\pi}{4}\right) \hat{y} \right], \quad (21)$$

where β is the apex angle and \hat{x}, \hat{y} are unit vectors along the crystal directions a, b . The length $a = \sqrt{\Phi_0/B \sin \beta}$ relates to the VL size in real space, where Φ_0 is the flux quantum and B is the magnetic induction.

The free energy density can be expressed as a sum over the reciprocal lattice, see e.g. [16]:

$$F = \frac{B^2}{8\pi} \sum_{\mathbf{G} \neq 0} \left(\frac{e^{-G^2/G_m^2}}{1 + G^2 \lambda_{ab}^2} + \eta \frac{G_x^4 + G_y^4}{G^4} e^{-G^2/G_e^2} \right), \quad (22)$$

where we introduced two cutoffs, G_m and G_e , for the magnetic and elastic contributions in divergent sums. Here, the factor

$$\eta = \frac{16\pi^3 S_0^2 d}{\Phi_0^2 D^2} \left(\lambda_1 + \lambda_2 - \frac{d}{2\lambda_3} \right), \quad (23)$$

characterizes the strain contribution to the inter-vortex interaction. Here λ_{ab} and λ_c , ξ_{ab} , ξ_c discussed below are the

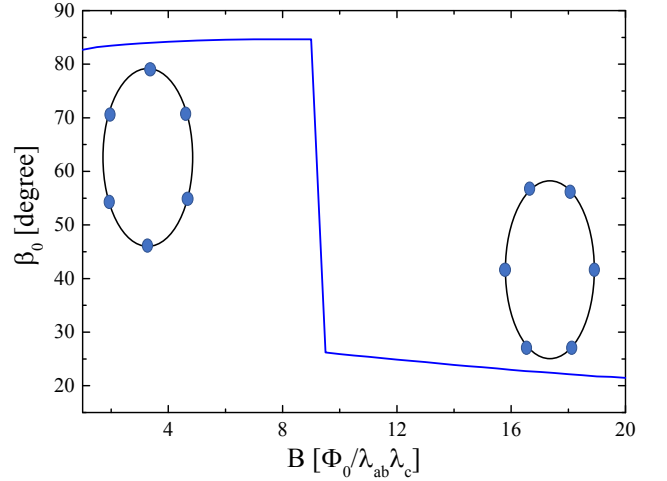


FIG. 2. (color online) The apex angle β of the rhombic unit cell for $\mathbf{B} \perp \mathbf{c}$. Insets are the sketches of the corresponding Bragg peaks of maximum intensity in the momentum space at low and high fields. Here $\eta_X = 0$, $\eta_Y = 0.002$, $\tilde{\gamma} = 2$, $\gamma = 2$ and $\bar{\kappa} = 30$.

anisotropic London penetration depth and superconducting coherence length respectively.

We roughly estimate $\eta \sim S_0^2 / \Phi_0^2 \tilde{\lambda}$, where $\tilde{\lambda}$ is the order of magnitude of elastic constants. Here $S_0 \sim \tilde{\lambda} \xi_{ab}^2 \frac{H_c^2}{T_c} \frac{dT_c}{dp} \left(\ln \frac{\lambda_{ab}}{\xi_{ab}} \right)^2$. For $dT_c/dp \approx 1$ K/GPa, $H_c = 1$ T and $\tilde{\lambda} \sim 10^{12}$ erg/cm³, we obtain $\eta \sim 5 \times 10^{-4}$ [6].

We perform numerical summation in Eq. (22) to obtain β corresponding to minimum energy for a given magnetic field. We find that the rhombus with diagonal along $[100]$ has lower energy when $\eta > 0$. The results for $\eta = 0.005$ is shown in Fig. 1. At low fields where the separation between vortices

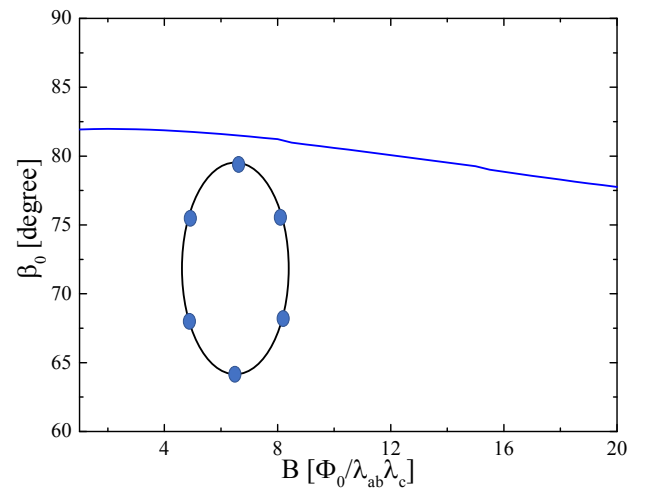


FIG. 3. (color online) The apex angle β of the rhombic unit cell when for $\mathbf{B} \perp \mathbf{c}$. Inset is a sketch of the corresponding Bragg peaks of maximum intensity in the momentum space. Here $\eta_X = 0.001$, $\eta_Y = 0$, $\tilde{\gamma} = 2$, $\gamma = 2$ and $\bar{\kappa} = 30$.

is larger than λ_{ab} , the long-range strain induced interaction is dominant, therefore the square VL is stabilized. In intermediate fields, the magnetic interaction favors a triangular VL. The triangular VL then evolves continuously to a square lattice for a high vortex density, because the long-range elastic interaction is $\propto B^2$, whereas the large field London interaction energy goes as $\Phi_0 B / \lambda_L^2$. Hence, at large B the elastic contribution is dominant and the VL follows the crystal symmetry. For a larger η , the intermediate region for triangular structures VL shrinks, and eventually disappears for a sufficiently strong elastic interaction.

We have introduced a cutoff $G_m = 1/\xi_{ab}$ for G to exclude distances shorter than the core size ξ_{ab} (or $G > 1/\xi_{ab}$) by adding a damping factor $\exp(-G^2 \xi_{ab}^2)$ in Eq. (22), the standard procedure in the London approximation.

Since the source of the strain generated by vortex can be related not only to the vortex core, but to the supercurrents around it [9], the cutoff G_e in the elastic part of energy (22) can differ from the London cutoff G_m . Numerical results and the threshold field to stabilize the square lattice depend on the cutoff G_e as shown in Fig. 1. Nevertheless, the qualitative feature that the square VL is favored by the strain induced interaction is robust against the cutoff.

As is seen from Eq. (15), the VL configuration for a negative η is related to the corresponding positive η by rotation of the whole lattice by $\pi/4$. Therefore in this case the diagonal of the rhombic unit cell is along the [110].

Next, we consider vortex lines in the ab plane. Because of the anisotropic penetration depth, the VL is no longer hexagonal in the absence of strain. Taking the crystal anisotropy into account, the London contribution to the energy density is

$$F_m = \frac{B^2}{8\pi} \sum_{G \neq 0} \frac{\exp(-G_X^2 \xi_{ab}^2 - G_Y^2 \xi_c^2)}{1 + G_Y^2 \lambda_{ab}^2 + G_X^2 \lambda_c^2}, \quad (24)$$

and the contribution due to strain is

$$F_e = 2 \left(\frac{\pi B d S_0}{\Phi_0 D_2} \right)^2 \sum_{G \neq 0} \frac{f_X (D_1 D_2^{-1} G_X)^4 + f_Y G_Y^4}{[(D_1 D_2^{-1} G_X)^2 + G_Y^2]^2} e^{-G_X^2 \xi_{ab}^2 - G_Y^2 \xi_c^2}. \quad (25)$$

We rescale the length $G_Y \lambda_{ab} \rightarrow G_Y$ and $G_X \lambda_c \rightarrow G_X$, such that F_m becomes isotropic. The total energy density then reads as

$$F = \frac{B^2}{8\pi} \sum_{G \neq 0} e^{-G^2/\bar{\kappa}^2} \left[\frac{1}{1 + G^2} + \frac{\eta_X (G_X^2 \bar{\gamma}^{-2})^2 + \eta_Y G_Y^4}{(G_Y^2 + G_X^2 \bar{\gamma}^{-2})^2} \right] \quad (26)$$

with $\bar{\kappa} = \lambda_{ab}/\xi_c = \lambda_c/\xi_{ab}$ and $\bar{\gamma}^{-2} = D_1 D_2^{-1} \lambda_{ab}^2 / \lambda_c^2$ [19].

To check possible VL structure transitions, we take

$$\eta_{X,Y} \equiv 16\pi^3 \left(\frac{dS_0}{\Phi_0 D_2} \right)^2 f_{X,Y}, \quad (27)$$

as free parameters to obtain the equilibrium vortex configurations. We consider the VL rhombic unit cell with the diagonal along the X axis in the rescaled frame. The apex angle is β . The apex angle β_0 , before rescaling is given by $\tan(\beta_0/2) = \tan(\beta/2)/\gamma$ with $\gamma = \lambda_c/\lambda_{ab}$. Below we present the results for two typical parameters.

The equilibrium apex angle β_0 for $\eta_X = 0$, $\eta_Y = 0.002$, $\gamma = 2$ and $\bar{\gamma} = 2$ is shown in Fig. 2. At low fields $\beta_0 \approx 83^\circ$ and it drops to about $\beta_0 \approx 24^\circ$ at high fields. The jump indicates a reorientation of the VL upon increasing field. To relate to the neutron scattering measurements, we depict in the inset the reciprocal unit vector in the first shell for both VL orientations. This reorientation resembles the one observed in CeCoIn₅ for field along the [110] direction.

The results for $\eta_X = 0.001$, $\eta_Y = 0$, $\gamma = 2$ and $\bar{\gamma} = 2$ are displayed in Fig. 3. The apex angle depends weakly on the field and there is no reorientation, similar to behavior observed in CeCoIn₅ for field along the [100] direction. We note that since η_X and η_Y depend on the field angle through $\Lambda_{\alpha\beta\gamma\eta}(\varphi)$, it is possible that VL reorients when field rotates in the ab plane.

IV. DISCUSSION

We expect stabilization of the square VL and the reorientation of VLs due to vortex-induced strain to occur in a broad class of materials and in heavy fermion superconductors, in particular.

In heavy fermion superconductors, such as CeCoIn₅ and CeRhIn₅, T_c depends strongly on pressure, pointing to a possible strain-induced inter-vortex interactions which affect the VL structures. For CeCoIn₅, $\partial T_c / \partial p \approx 0.3$ K/GPa at the ambient pressure. In a large family of Fe-based materials, this derivative is larger yet and depends on doping; in some of them $\partial T_c / \partial p$ can be one or two orders of magnitude larger [10].

The small angle neutron scattering data on VLs in CeCoIn₅ are available [11–13]. At low fields along the c axis and low temperatures, the VL is triangular (rhombic). Upon increasing field, the VL becomes square. With further increase of the magnetic field, the VL becomes triangular again.

One possible explanation to the triangular-square VL transition in CeCoIn₅ could be the strain-induced intervortex interaction. It is worth noting that strain-induced interactions are not the only possible mechanism to stabilize the square lattice. It may also be due to non-local corrections to the London interactions due to the basic nonlocality of current-field relation in superconductors, as has been demonstrated theoretically and experimentally for borocarbides [2]. However, the high-field square-to-triangle transition cannot be explained by the nonlocal effects. It can be caused by fluctuations of vortices near the upper critical field H_{c2} [20] or by the strong Pauli pair breaking [21].

On the other hand, one can argue that within the magneto-elastic scenario considered here, the vortex induced strains disappear faster than the standard inter-vortex interaction when the field increases toward $H_{c2}(T)$. The strain-induced interaction has been estimated in [4]:

$$F_e \sim \tilde{\lambda} \left(\frac{\Phi_0 B}{16\pi^2 \lambda_L^2 T_c} \frac{\partial T_c}{\partial p} \right)^2. \quad (28)$$

The London interaction energy density in intermediate fields

is

$$F_m \sim \frac{\Phi_0 B}{32\pi^2 \lambda_L^2} \ln\left(\frac{H_{c2}}{B}\right). \quad (29)$$

As T increases toward $T_c(B)$ at a fixed B , $F_e \propto 1/\lambda_L^4$ decreases faster than $F_m \propto 1/\lambda_L^2$. As a result VL favors the triangular lattice because of the dominant magnetic interaction. Hence, both the triangle-to-square evolution of VLs and the square-to-triangle transition on approach to H_{c2} can, in principle, be attributed to the existence and variation of the vortex induced strains.

Experimentally, for CeCoIn₅ in the field parallel to [110], the VL rotates near $B \approx 8$ T, similar to that shown in Fig. 2. For field along [100], the observed VL deforms weakly, which is akin to behavior in Fig. 3. Unfortunately, direct comparison between the theory and experiment is not possible at the moment because the elastic moduli of CeCoIn₅ are not known.

To summarize, we have studied vortex lattice configurations in tetragonal superconductors taking into account the strain field created by vortices. When vortex lines are directed along the c axis and for a weak vortex-strain coupling, the square vortex lattice is stabilized both at high and low vortex densities, while the triangular vortex lattice is favored at intermediate densities. In the presence of a strong vortex-strain coupling, the square vortex lattice may be favored in the whole field region. When vortex lines lie in the ab plane, the vortex lattice can reorient with increasing magnetic field. Our results are in qualitative agreement with the vortex evolution and transitions in CeCoIn₅.

V. ACKNOWLEDGEMENTS

The authors thank Lev Bulaevskii, Roman Movshovich, Leonardo Civale, Duk Y. Kim, and Ian Fisher for helpful discussions. The work by SZL was carried out under the auspices of the U.S. DOE Contract No. DE-AC52-06NA25396 through the LDRD program. VGK was supported by the U.S. Department of Energy, Office of Science, Basic Energy Sciences, Materials Sciences and Engineering Division. The Ames Laboratory is operated for the U.S. DOE by Iowa State University under Contract No. DE-AC02-07CH11358.

Appendix A: Elastic moduli in the rotated frame

With the help of Eq. (5) we evaluate the elastic moduli in the vortex frame when the vortex axis Z is in the ab plane of a tetragonal crystal. The azimuthal angle φ is the angle between the Z and a axes and the axis Y coincides with the c axis.

$$\begin{aligned} \Lambda_{XXXX} &= [3\lambda_1 + \lambda_2 + 2\lambda_3 + (\lambda_1 - \lambda_2 - 2\lambda_3) \cos(4\varphi)]/4, \\ \Lambda_{XXXZ} &= (\lambda_1 - \lambda_2 - 2\lambda_3) \sin(4\varphi)/4, \\ \Lambda_{XXZZ} &= [\lambda_1 + 3\lambda_2 - 2\lambda_3 + (-\lambda_1 + \lambda_2 + 2\lambda_3) \cos(4\varphi)]/4, \\ \Lambda_{XZZZ} &= [\lambda_1 - \lambda_2 + 2\lambda_3 + (-\lambda_1 + \lambda_2 + 2\lambda_3) \cos(4\varphi)]/4, \\ \Lambda_{XZZZ} &= (-\lambda_1 + \lambda_2 + 2\lambda_3) \sin(4\varphi)/4, \end{aligned}$$

$$\text{and } \Lambda_{XXYY} = \Lambda_{YYZZ} = \lambda_5, \Lambda_{YYYY} = \lambda_4, \Lambda_{XYXY} = \Lambda_{YZYZ} = \lambda_6.$$

-
- [1] A. A. Abrikosov, "On the magnetic properties of superconductors of the second group," *Soviet Physics JETP-USSR* **5**, 1174–1183 (1957).
 - [2] V. G. Kogan, M. Bullock, B. Harmon, P. Miranovic-acute, Lj. Dobrosavljevic-acute Grujic-acute, P. L. Gammel, and D. J. Bishop, "Vortex lattice transitions in borocarbides," *Phys. Rev. B* **55**, R8693–R8696 (1997).
 - [3] Ian Affleck, Marcel Franz, and M. H. Sharifzadeh Amin, "Generalized london free energy for high- T_c vortex lattices," *Phys. Rev. B* **55**, R704–R707 (1997).
 - [4] V. G. Kogan, L. N. Bulaevskii, P. Miranović, and L. Dobrosavljević-Grujić, "Vortex-induced strain and flux lattices in anisotropic superconductors," *Phys. Rev. B* **51**, 15344–15350 (1995).
 - [5] P. Miranović, Lj. Dobrosavljević-Grujić, and V. G. Kogan, "Ginzburg-landau theory of vortex lattice structure in deformable anisotropic superconductors," *Phys. Rev. B* **52**, 12852–12857 (1995).
 - [6] V. G. Kogan, "Elastic contribution to interaction of vortices in uniaxial superconductors," *Phys. Rev. B* **88**, 144514 (2013).
 - [7] V. G. Kogan, "Vortex-induced strain and magnetization in type-II superconductors," *Phys. Rev. B* **87**, 020503 (2013).
 - [8] D. Domínguez, L. Bulaevskii, B. Ivlev, M. Maley, and A. R. Bishop, "Interaction of vortices with ultrasound and the acoustic faraday effect in type-II superconductors," *Phys. Rev. B* **53**, 6682–6692 (1996).
 - [9] A. Cano, A. P. Levanyuk, and S. A. Minyukov, "Elasticity-driven interaction between vortices in type-II superconductors," *Phys. Rev. B* **68**, 144515 (2003).
 - [10] E. Gati, S. Köhler, D. Guterding, B. Wolf, S. Knöner, S. Ran, S. L. Bud'ko, P. C. Canfield, and M. Lang, "Hydrostatic-pressure tuning of magnetic, nonmagnetic, and superconducting states in annealed Ca(Fe_{1-x}Co_x)₂As₂," *Phys. Rev. B* **86**, 220511 (2012).
 - [11] Andrea D. Bianchi, Michel Kenzelmann, Lisa DeBeer-Schmitt, Jon S. White, Edward M. Forgan, Joel Mesot, Markus Zolliker, Joachim Kohlbrecher, Roman Movshovich, Eric D. Bauer, John L. Sarrao, Zachary Fisk, Cedomir Petrović, and Morten Ring Eskildsen, "Superconducting Vortices in CeCoIn₅: Toward the Pauli-Limiting Field," *Science* **319**, 177–180 (2008).
 - [12] J. S. White, P. Das, M. R. Eskildsen, L. DeBeer-Schmitt, E. M. Forgan, A. D. Bianchi, M. Kenzelmann, M. Zolliker, S. Gerber, J. L. Gavilano, J. Mesot, R. Movshovich, E. D. Bauer, J. L. Sarrao, and C. Petrovic, "Observations of Pauli paramagnetic effects on the flux line lattice in CeCoIn₅," *New Journal of Physics* **12**, 023026 (2010).
 - [13] P. Das, J. S. White, A. T. Holmes, S. Gerber, E. M. Forgan, A. D. Bianchi, M. Kenzelmann, M. Zolliker, J. L. Gavilano, E. D. Bauer, J. L. Sarrao, C. Petrovic, and M. R. Eskildsen, "Vortex lattice studies in CeCoIn₅ with $H \perp c$," *Phys. Rev. Lett.* **108**, 087002 (2012).

- [14] L. D. Landau and E. M. Lifshitz, *Theory of Elasticity* (Butterworth-Heinemann, Oxford, 1986).
- [15] V. G. Kogan, “London approach to anisotropic type-II superconductors,” *Phys. Rev. B* **24**, 1572–1575 (1981).
- [16] L. J. Campbell, M. M. Doria, and V. G. Kogan, “Vortex lattice structures in uniaxial superconductors,” *Phys. Rev. B* **38**, 2439–2443 (1988).
- [17] John Bardeen and M. J. Stephen, “Theory of the motion of vortices in superconductors,” *Phys. Rev.* **140**, A1197–A1207 (1965).
- [18] L. D. Landau and E. M. Lifshitz, *Electrodynamics of Continuous Media* (Pergamon Press, Oxford, 1984).
- [19] The equality $\lambda_{ab}/\xi_c = \lambda_c/\xi_{ab}$ holds only if the anisotropies of the penetration depth and of the coherence length are the same $\lambda_{ab}/\lambda_c = \xi_{ab}/\xi_c$, which is in general true only at T_c . At low T ’s, this anisotropies may differ substantially; e.g., for MgB_2 at $T = 0$, $\gamma_\lambda = \lambda_c/\lambda_{ab} \approx 1$, whereas $\gamma_\xi = \xi_{ab}/\xi_c \approx 6$. Still, we keep $\gamma_\lambda = \gamma_\xi$ not to make our formulas too cumbersome.
- [20] A. Gurevich and V. G. Kogan, “Effect of fluctuations on vortex lattice structural transitions in superconductors,” *Phys. Rev. Lett.* **87**, 177009 (2001).
- [21] Norihito Hiasa and Ryusuke Ikeda, “Instability of square vortex lattice in d -wave superconductors is due to paramagnetic depairing,” *Phys. Rev. Lett.* **101**, 027001 (2008).